Title
Optic Nerve Crush Induces Selective Retinal Ganglion Cell Degeneration in the Rat Retina /

Permalink
https://escholarship.org/uc/item/48x9b40q

Author
Ahn, Daniel Sung J.

Publication Date
2013

Peer reviewed|Thesis/dissertation

UNIVERSITY OF CALIFORNIA, SAN DIEGO

Optic Nerve Crush Induces Selective Retinal Ganglion Cell Degeneration in the
Rat Retina

A Thesis submitted in partial satisfaction of the requirements for the degree
Master of Science

in

Biology

by

Daniel Sung J Ahn

Committee in charge:

      Professor E.J. Chichilnisky, Chair
      Professor Andrew D. Huberman
      Professor James D. Lindsey

2013

The Thesis of Daniel Sung J Ahn is approved and it is acceptable in quality and form for publication on microfilm:

_____

_____

_____

Chair

University of California, San Diego

2013

TABLE OF CONTENTS

LIST OF FIGURES

ACKNOWLEDGMENTS

I would like to thank Dr. E.J. Chichilnisky for being an excellent advisor. He has been a constant source of guidance and wisdom ever since I joined the lab. Thanks to his support, my dream to pursue a wonderful career in medicine is a reality. I am forever indebted.

I would like to thank Dr. Greg D. Field for being the best mentor in the world. My time in this lab has been meaningful because of his willingness to teach, and guide me patiently.

I would also like to thank Dr. Fumitaka Osakada for being a wonderful mentor. He has been incredibly generous with his time and knowledge.

Now, I would like to thank all the past and present members of the Chichilnisky lab: Dr. Martin Greschner, Dr. Peter Li, Dr. Lauren Jepson, Alexander Heitman, Geoffrey Weiner, Daniela Amado, and Clare Hulse. In particular, I would like to thank Geoffrey Weiner for being a great friend and mentor. I look forward to our epic days in Doctors Without Borders.

I would also like to thank Dr. James D. Lindsey and Dr. Andrew D. Huberman for serving on my master thesis committee.

Last, but not least, I would like to thank my parents who have sacrificed immensely on my behalf.

ABSTRACT OF THE THESIS

Optic Nerve Crush Induces Selective Retinal Ganglion Cell Degeneration in the
Rat Retina

by

Daniel Sung J Ahn

Master of Science in Biology

University of California, San Diego, 2013

Professor E.J. Chichilnisky, Chair

Glaucoma is a common cause of blindness characterized by the

degeneration of optic nerve and retinal ganglion cells (RGC). A longstanding

question in glaucoma research is whether certain RGC types are more

susceptible to glaucoma than other RGC types. It is well understood that the

mammalian retina contains a diverse population of RGCs – humans have ~20

distinct RGC types; each cell type exhibits unique morphological and physiological properties. Given the diversity of RGC types in the retina, it is plausible that different cell types respond differently to glaucoma and thus, certain cell types may degenerate at earlier time points than others. Determining whether specific RGC types degenerate at earlier time points can have important clinical impact on early detection and treatment of glaucoma.

To study whether certain RGC types degenerate at earlier time points, we used a large-scale multi-electrode system to record the action potentials of hundreds of RGCs simultaneously in healthy and optic nerve crushed rat retinas. ~9 distinct RGC types were identified in the healthy rat retina based on unique light response and intrinsic spiking properties. The results in the healthy rat retina were compared to the optic nerve crushed rat retina to assess whether certain RGC types degenerated at earlier time points following optic nerve crush. The current results show that 2 RGC types degenerate selectively at ~10 days after optic nerve crush.

Introduction:

Glaucoma is a common cause of blindness characterized by gradual degeneration of the optic nerve and retinal ganglion cells (RGC), which send visual information to the brain. Elevated intraocular pressure (IOP) is frequently associated with optic nerve and RGC degeneration; however, the exact cause or mechanism of the disease remains unclear [1-5].

An important, longstanding question in glaucoma research is whether different types of RGCs degenerate preferentially at different time points. The mammalian retina contains a diverse population of RGC types; it is well understood that humans have ~20 morphologically distinct RGC types [6-7] and recent studies have shown that rats have ~16 morphologically distinct RGC types [8]. Given the diversity of cell types in the retina, it is possible that different RGC types respond differently to glaucomatous stress such as elevated IOP. Determining whether certain RGC types degenerate at earlier time points can improve our understanding of the fundamental disease mechanism of glaucoma and give important clues for clinicians to identify early signs of glaucoma, contribute to developing cell-type specific diagnostic tests and treat patients sooner using available therapies.

A number of studies have attempted to answer whether certain RGC types are more susceptible to glaucoma. Previous studies have shown that large optic nerve fibers and RGCs are more susceptible to glaucoma in monkey and human eyes [9-11]. Shou et al. showed that α RGCs undergo more severe dendritic

1

retraction than β RGCs in elevated IOP model of the cat retina [12]. More

recently, Feng et al. showed that ON-response RGCs degenerate more rapidly

than the ON-OFF-response RGCs in elevated IOP model of the mouse retina

[13]. However, other studies have also suggested non-selective RGC death in

experimental glaucoma [14-16].

To study whether different RGC types degenerate at different time points,

we used a large-scale multi-electrode system to record the action potentials of

hundreds of RGCs simultaneously in healthy and optic nerve crushed rat retinas.

This method allowed us to identify and compare ~5-9 RGC types based on

unique light response and intrinsic spiking properties in the healthy and optic

nerve crushed rat retinas [17]. The current results suggest that 1 OFF-response

and 1 ON-response cell types degenerate at ~10 days after optic nerve crush

treatment.

Methods:

Animals and Retina Dissection:

Adult Long Evans rats weighing ~350-400 g were used for both wild-type and optic nerve crushed retina recordings. The optic nerve crushed rats had 1 eye crushed and the other untreated; these animals were obtained from Dr. James D. Lindsey (UCSD Shiley Eye Center). All procedures followed the Salk Institute Guidelines for the care and use of animals.

The preparation of the optic nerve crushed rat conformed to the following procedures. The animal was anesthetized by intraperitoneal injection of ketamine (100mg/kg) and xylazine (10 mg/kg). Limbal conjunctival peritomy was performed in the temporal region and was gently peeled back to allow access to the posterior region of the globe. The optic nerve was then exposed through a small window made between the surrounding muscle bundles and fatty tissue by gentle blunt dissection. Care was taken not to damage muscles or the blood vessels. At a site approximately 1 mm posterior to the globe, the optic nerve was clamped using a pair of self-closing tweezers (Dumant No. 5; Ted Pella Inc., Redding, CA) for 5 seconds. After this procedure, antibiotic ointment was applied to the surgical site. In the postoperative period, the rat exhibited normal eating and drinking behavior.

All rats were dark-adapted for ~30 minutes or more prior to dissection and dissection was performed under infrared and red light. Ketamine and xylazine cocktail anesthesia was used to anesthetize animals prior to decapitation. After

decapitation, a healthy eye (control) and/or optic nerve crushed eye (treated) was enucleated. A razor blade was used to create a small incision posterior to the ora serrata and the eyeball was placed in Ames solution (Sigma, St. Louis, MO) for hemissection and vitrectomy. Following complete removal of the vitreous humor, the eyecup was transferred to a larger pinning dish containing oxygenated Ames solution for orientation based on visible vasculature. All retina pieces were isolated from the dorsal region of the eyecup, ~2.5 mm from the optic nerve to reduce variability across preparations. Prior to placing the retina over the array, the retina was immersed in ames solution containing 10 μg/mL of lectin peanut agluttinin (PNA) for fluorescent labeling of vasculature; fluorescent images of the retinal vasculature were taken at the end of all recordings to determine the orientation of the retina with respect to the electrode array.

Multi-electrode Array Recordings:

All electrophysiology recordings were done on a planar multi-electrode array containing 512 individual electrodes in a 16x32 arrangement; each electrode is 5 μm in diameter and spaced 60 μm from neighboring electrodes. The full array covers ~1800 x 900 μm^2 surface area.

A live isolated retina piece was placed over the electrode array with the ganglion cell layer facing the electrodes. A dialysis membrane was used to stabilize the retina piece over the electrodes from the photoreceptor side. The

retina was then continuously perfused with oxygenated Ames solution (95% O_2, 5% CO_2; 7.4 pH) at 33 C.

Once the retina was stabilized over the electrodes, visual stimuli were shown from the bottom of the mostly transparent array, and focused on the photoreceptors to elicit action potentials from RGCs. The action potentials of RGCs were recorded on individual electrodes as voltage traces; these voltage traces were digitized at 20 kHz and saved for off-line analysis.

Visual Stimulus:

The isolated retina pieces were shown a focused spatiotemporal white noise stimulus from a cathode-ray tube monitor (CRT) refreshing at 120 Hz. The spatiotemporal white noise stimulus was composed of a lattice of square pixels flickering black and white light independently and randomly over space and time. The visual stimulus was shown through the bottom of the mostly transparent array, centered over the electrodes and focused on the photoreceptors.

Spike Sorting:

Once the raw voltage traces were saved for off-line analysis, the action potentials of RGCs were identified using previously described methods [17-18]. First, action potentials had to cross an amplitude threshold to be identified as spikes. The candidate spikes were then represented as a waveform on the seed electrode as well as neighboring electrodes and spike clusters were formed via

principal component analysis (PCA). Spike clusters were associated with candidate neurons if the clusters exhibited refractory periods; spike clusters exhibiting refractory period violations were removed. Duplicate spike clusters arose from 2 or more nearby electrodes recording action potentials from the same RGC; duplicates were removed using temporal cross-correlation.

RF Characterization:

The receptive field properties of recorded RGCs were characterized by the spike-triggered average method, which is the average of stimulus preceding a neuronal action potential. For every spike identified, 500 ms of preceding stimulus was averaged to characterize the region in space over which changes in stimulus intensity drove neuronal spiking and the dynamics with which this occurred.

Electrophysiological Image:

Polyaxonal amacrine cells were identified based on the electrophysiological image (EI), which was described previously [17]. Briefly, the spike-triggered average electrical image was computed for each neuron identified. Each time a neuron fired a spike, the voltage waveform was saved for 0.5 ms preceding the neuronal spike and few milliseconds after the spike on each electrode; saved spike waveforms were averaged in each of the electrodes. The waveforms were inspected for somatic, dendritic, and axonal kinetic signatures.

The EI of a typical RGC exhibited signal propagation in one direction through the putative cell body and single axon. On the other hand, the EI of an amacrine cell exhibited signal propagation in multiple directions with signals emanating from the putative cell body through multiple axons.

Classification of RGC Types:

Custom software was used to classify 9 different RGC types based on the information shown in figures 1 and 2: (1) Spatial RFs; (2) Response time courses and (3) Autocorrelation functions of neuronal spiking. Cells were plotted on 2-dimensional PC plots to represent the distinguishing features of each cell; a point in the plot represented each cell. Using the PC plots, the cells were first divided based on their responses to increment and decrement in light – these were classified as ON and OFF cells, respectively (not shown) and classified into cell types by drawing distinct clusters as shown below.
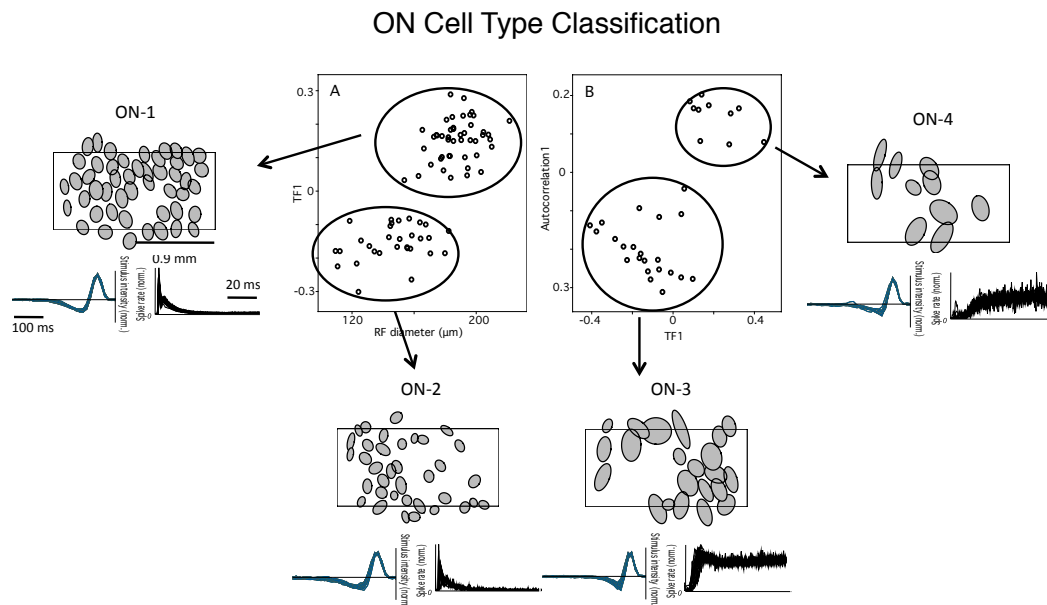
Figure 1. ON cell type classification. Each cell is represented by a point in the cluster plot. A. The classification plot represents each cell by weight of the response time course first principal component as a function of the receptive field diameter. Based on this information, ON-1 and ON-2 cells are identified. B. The classification plot represents each cell by weight of the autocorrelation first principal component as a function of the response time course first principal component. Based on this information, ON-3 and ON-4 cells are identified.

Figure 1 shows a typical example of how 4 distinct ON cell types were identified. Plot A shows the ON-1 and ON-2 cells represented in a PC plot showing the weight of the response time course first principal component as a function of the receptive field diameter. Plot B shows the ON-3 and ON-4 cells represented in a PC plot showing the weight of the autocorrelation first principal component as a function of the weight of the response time course first principal component. Despite accounting for only 2 distinguishing features per classification plot (i.e. TF1 vs. RF diameter), cells within each cell type exhibit strikingly similar spatial RFs, response time courses, and autocorrelation

functions. Moreover, these same features are strikingly distinct among different cell types. This is also true among the OFF cell types.
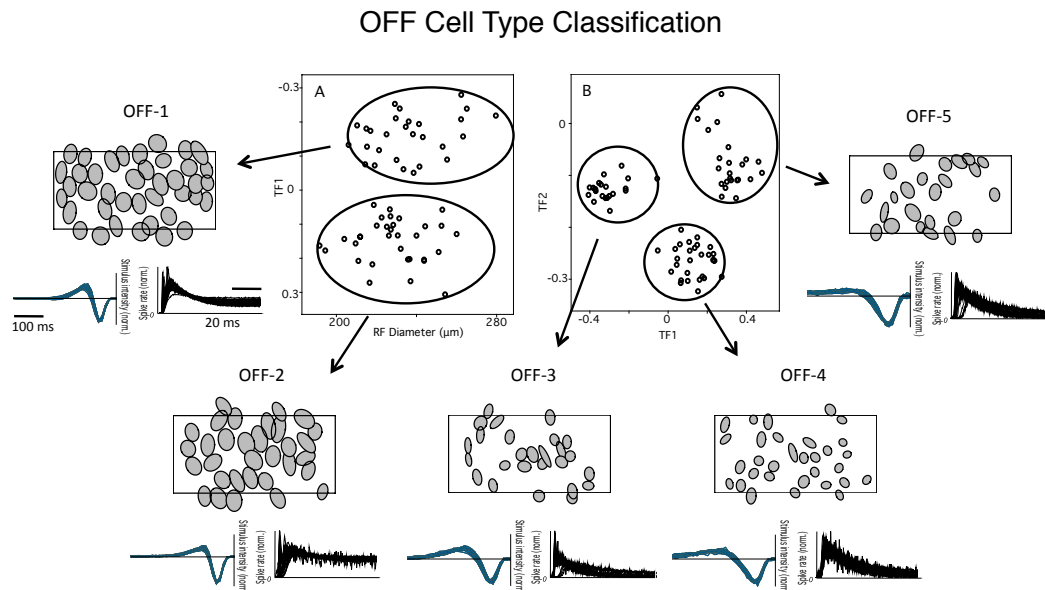
OFF Cell Type Classification

Figure 2. OFF cell type classification. A. The classification plot represents each cell by weight of the response time course first principal component as a function of the receptive field diameter. B. The classification plot represents each cell by weight of the response time course second principal component as a function of the response time course first principal component.

Figure 2 shows a typical example of how 5 distinct OFF cell types were identified. Plot A shows the OFF-1 and OFF-2 cells represented in a PC plot showing the weight of the response time course first principal component as a function of receptive field diameter. Plot B shows the OFF-3, OFF-4, and OFF-5 cells represented in a PC plot showing the weight of the response time course second principal component as a function of the weight of the response time course first principal component. Again, the light response features and autocorrelation functions are strikingly homogenous in cells within a cell type group and remarkably distinct among different cell types.
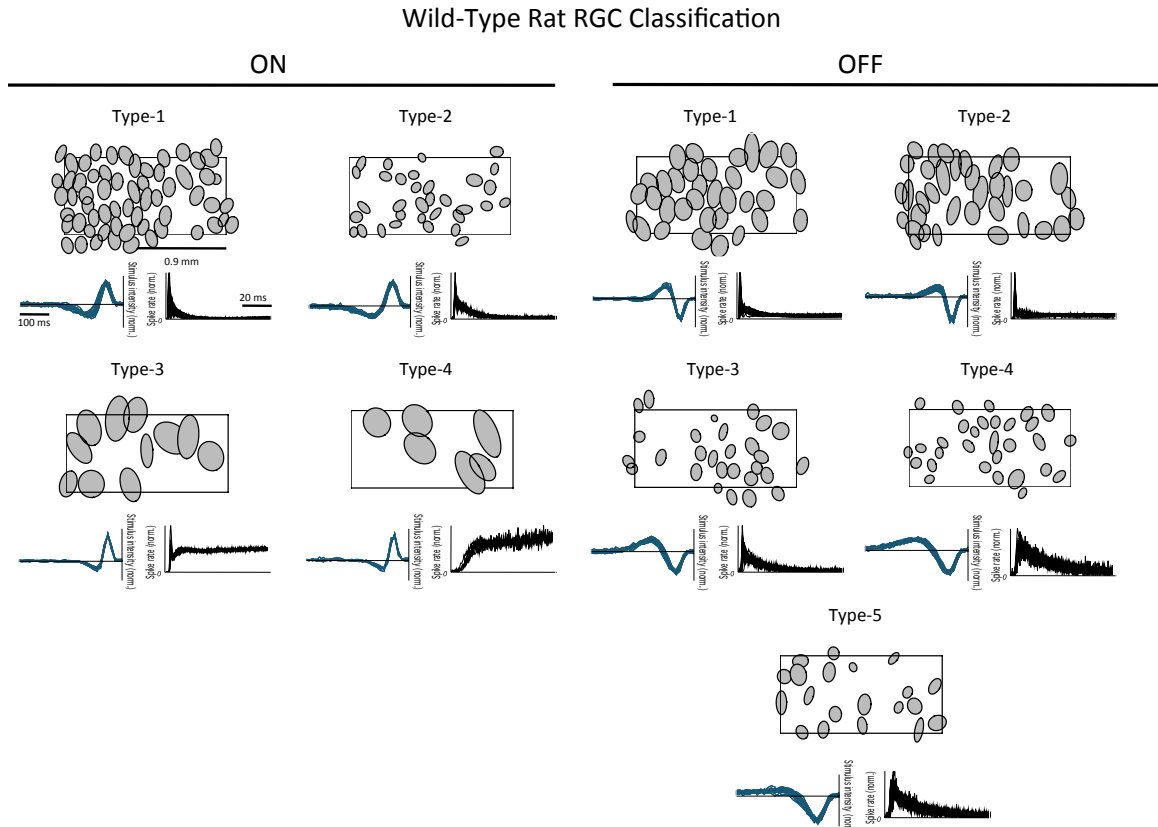
Results:

Figure 3. Cell type classification in the healthy rat retina. 9 distinct RGC types were classified based on responses to focused white noise stimuli (randomly flickering black and white checkerboard pattern). Each cell type was classified based on spatial receptive fields (top, center), response time courses (bottom left), and autocorrelation functions (bottom, right). The spatial receptive fields of RGCs are characterized by the spike-triggered average, in which neuronal action potentials are correlated to the visual stimulus. Each elliptical contour represents a light sensitive region associated with a single RGC. Response time courses represent the average intensity of the visual stimulus preceding a neuronal action potential, overlaid. Autocorrelation functions show intrinsic spiking properties of individual RGCs; the plots show the probability of spiking as a function of time following the occurrence of a spike at time 0.

To investigate RGC degeneration in optic nerve crushed rat retinas, 2 objectives were fulfilled using electrophysiology methods: First, RGC types were identified and classified in the healthy rat retina, and second, RGC types were identified and classified in the optic nerve crushed rat retina at different time

10

points following optic nerve crush. The results from the healthy and optic nerve crushed rat retinas were compared to assess whether some RGC types degenerated preferentially following optic nerve crush.

First, electrophysiology recordings were done on healthy rat retinas to identify and classify distinct RGC types. RGC types were classified based on distinct light response properties and intrinsic spiking properties (see Methods). Based on these criteria, each healthy retina recordings yielded up to ~9 different cell types as shown in figure 1. High quality experiments were difficult to achieve consistently; however, lower quality experimental data still yielded ~5 RGC types (ON Type 1-2; OFF Type 1-3) reliably across recordings. The primary difference between a high quality and low quality data was the signal-to-noise ratio of spikes. In higher quality data, neuronal spikes were robustly separated from background activity allowing for the light responses of each cell to be characterized clearly and more cells to be found in each recording; the opposite was true in lower quality recordings. In addition to RGCs, polyaxonal amacrine cells were identified based on the electrophysiological image (see Methods); amacrine cells exhibited signal propagation in multiple directions from the cell body through multiples axons.
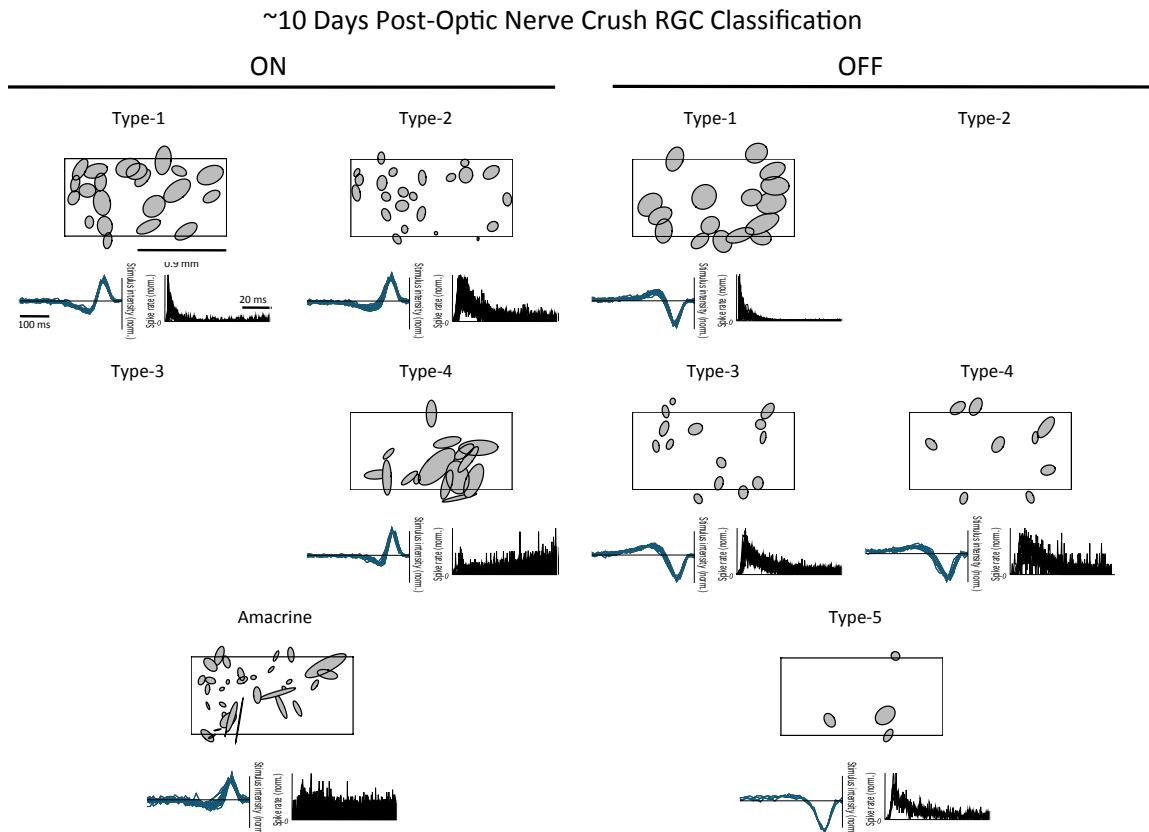
Figure 4. Cell type classification in ~10 days post-nerve crush rat retina. ON Type-3 and OFF Type-2 cells are unidentifiable by ~10 days following nerve crush treatment.

Once RGC types in the healthy rat retinas were established, electrophysiology recordings were done in optic nerve crushed rat retinas to identify and classify RGC types and to see whether some RGC types degenerated at earlier time points following optic nerve crush. In the optic nerve crushed retina, the results showed that 2 RGC types – ON type-3 and OFF Type-2 – were unidentifiable by ~10 days following nerve crush as shown in figure 2. Similar results were also seen in 2 additional recordings at ~10 days and ~11 days after nerve crush (see Appendix). These results suggest that selective RGC degeneration is plausible with possible implications for glaucoma.

~15 Days Post-Optic Nerve Crush RGC Classification
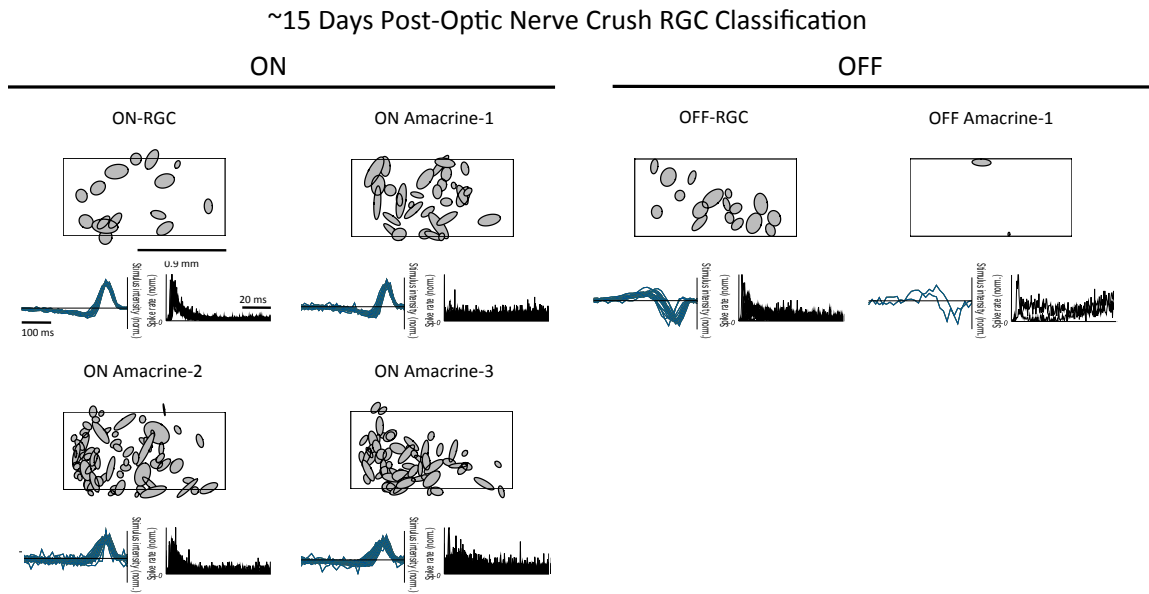
Figure 5. Cell type classification in ~15 days post-nerve crush rat retina.

Recordings were also done in retinas ~2 weeks after optic nerve crush as shown in figure 5. RGCs were difficult to identify by specific types at this time point. However, to our surprise, the data yielded many ON-response amacrine cells in addition to few OFF-response amacrine cells. Similar results were also found in 2 additional recordings at ~14 days and ~15 days post-optic nerve crush time points (see Appendix). These results suggest that many RGCs degenerate and cease to fire neuronal spikes at this time point allowing for signals from amacrine cells to be recorded at greater efficiency.

Discussion

        The goal of the current study was to examine whether some RGC types degenerated at earlier time points than other RGC types in the optic nerve crushed rat retina. Using a large-scale multi-electrode recording system, we found 2 distinct RGC types which were unidentifiable by ~10 days after optic nerve crush.

RGC Degeneration in Experimental Glaucoma

        It is unclear whether selective RGC degeneration occurs in glaucoma. In earlier studies, Quigley et al. and Glovinsky et al. reported that larger optic nerve fibers and RGCs degenerated more rapidly than smaller optic nerve fibers and RGCs in glaucoma eyes of monkeys and humans [9-11]. These results raised the possibility to target larger cell types for early detection of glaucoma. In another study, Shou et al. showed that α RGCs degenerated more severely than β RGCs by comparing dendritic structures (i.e. dendrite radii, lengths, bifurcations) of healthy and glaucoma eyes of cats [12]. Finally, Feng et al. showed that ON cells degenerated more rapidly than ON-OFF cells by comparing the dendritic field and soma sizes of ON cells and ON-OFF cells in the glaucoma eyes of mice [13]. These studies, however, have been largely limited to general observations of morphological changes of RGCs. In addition, the results from these studies have been questioned due to the difficulty of identifying distinct RGC types unequivocally [16].

The results from our study favor the idea that selective RGC degeneration occurs in glaucoma – the putative ON Type-3 and OFF Type-2 cells are unidentifiable by ~10 days following optic nerve crush while the other cell types retained relatively normal light responses. The limitation in our study, however, is that there is some uncertainty to whether OFF Type-1 or OFF Type-2 cells are being affected preferentially, and similarly, whether ON Type-3 or ON Type-4 cells are being affected preferentially because some RGCs exhibit physiological changes following axonal injuries. For example, by ~4 days after nerve crush treatment, the putative OFF Type-2 cells exhibit STA time courses, which are significantly less biphasic than the OFF Type-2 cells identified in healthy retinas; this trend continues at ~7-8 days following nerve crush treatment. In addition, by ~8 days after nerve crush treatment, the intrinsic firing properties of the putative OFF Type-2 cells begin to change with respect to the intrinsic firing properties of the OFF Type-2 cells in the healthy retinas. The changes in physiological properties induced by optic nerve crush treatment make it difficult to resolve which cell type (OFF Type-1 or OFF Type-2; ON Type-3 or ON Type-4) is being affected. This requires that we develop better ways to track physiological changes of each cell type more accurately over time. In addition, matching physiological cell type classification with anatomical cell type classification in the optic nerve crushed retina may be helpful to clarify which cell types degenerate preferentially.

Optic Nerve Crush Model vs. Elevated IOP Model

It is important to note the difference between the effects of elevated IOP and optic nerve crush on the optic nerve and RGCs. A study by Kalenykas et al. showed that elevated IOP mice after ~6 weeks exhibited 31% axon loss and no significant loss of RGC cell bodies whereas the optic nerve crush mice after ~9 days exhibited 98% axon loss and 64% loss of RGC cell bodies [19]. These results are unsurprising given that glaucoma in human patients typically result in gradual RGC degeneration occurring over months to years and is strongly correlated to elevated IOP. Given the drastic difference in the effects between these models, the next logical step in our research is to study RGC degeneration in an experimental elevated IOP model using current electrophysiology methods.

Significance

Studying how RGCs respond to optic nerve injury is an important prerequisite to understand the fundamental disease mechanism of glaucoma and to potentially improve our capacity to diagnose glaucoma early on. From our results, 3 conclusions can be made – (1) RGCs undergo selective physiological change at early stages of degeneration (OFF-2), (2) 2 RGCs are lost by 10 days after nerve crush (OFF-2, ON-3) and (3) The number of amacrine cells increase dramatically at late stages of degeneration. These conclusions suggest a few implications for glaucoma. First, selective degeneration seen in our results

introduces the possibility to probe certain cell types for early detection of

glaucoma. In particular, the early changes in light response dynamics in specific

cells (i.e. OFF-2) suggest the possibility of early diagnosis based on timing of

visual sensitivity. Second, the amacrine cells found in late stages of degeneration

(~15 days post-crush) suggest that nearly all RGCs have degenerated at this

time point. The increase in the number of amacrine cells may simply reflect the

idea that sick RGCs fire less spikes allowing for clear detection of amacrine cell

signals. This last point reinforces the need to improve early diagnosis techniques

to detect glaucoma early on and prevent irreversible vision loss occurring from

RGC death.

Appendix:

Wild-Type Rat RGC Classification #1
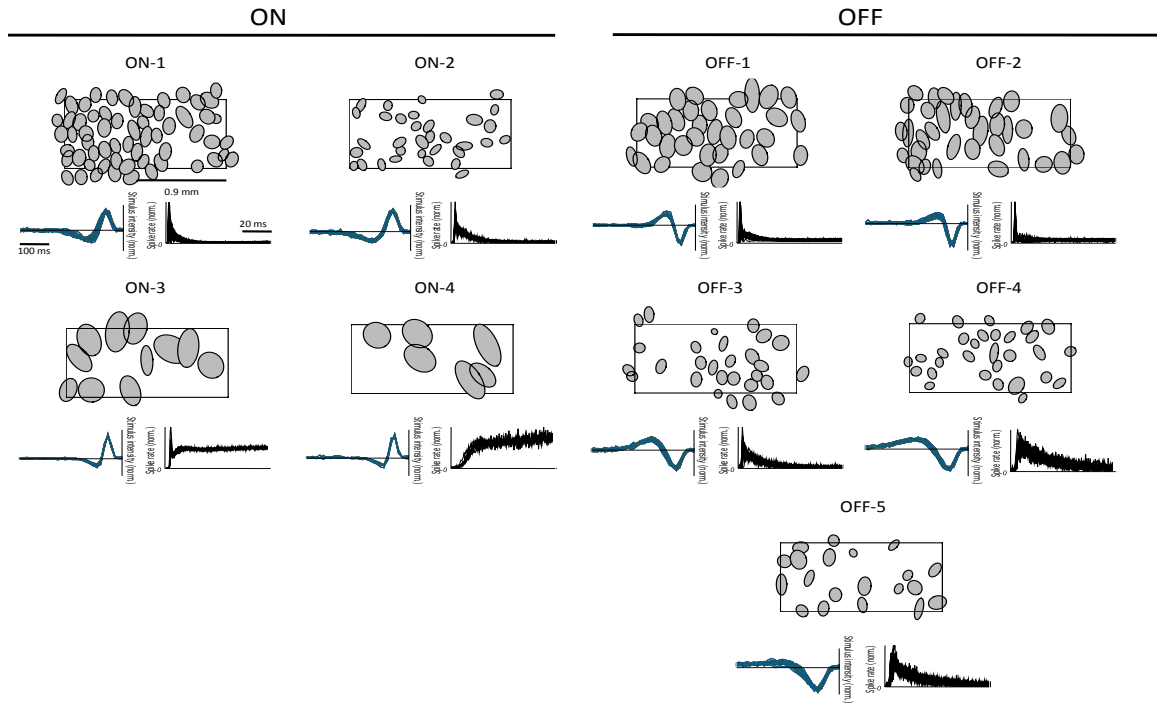
Wild-Type Rat RGC Classification #2
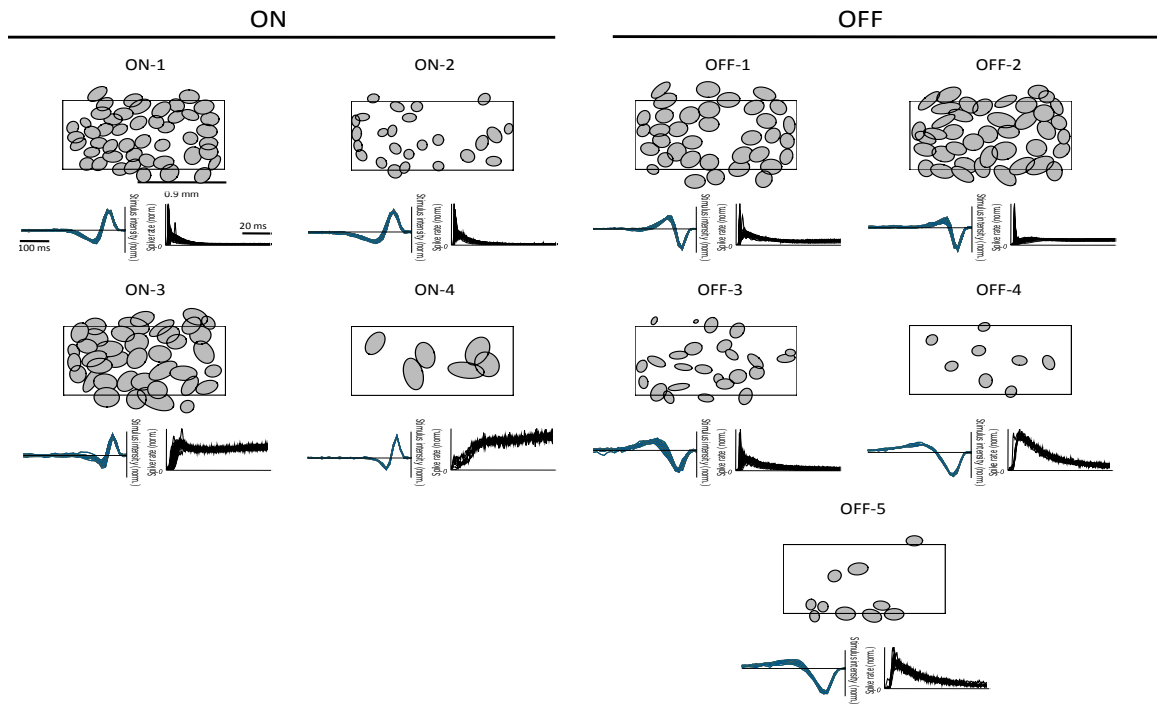
Wild-Type Rat RGC Classification #3
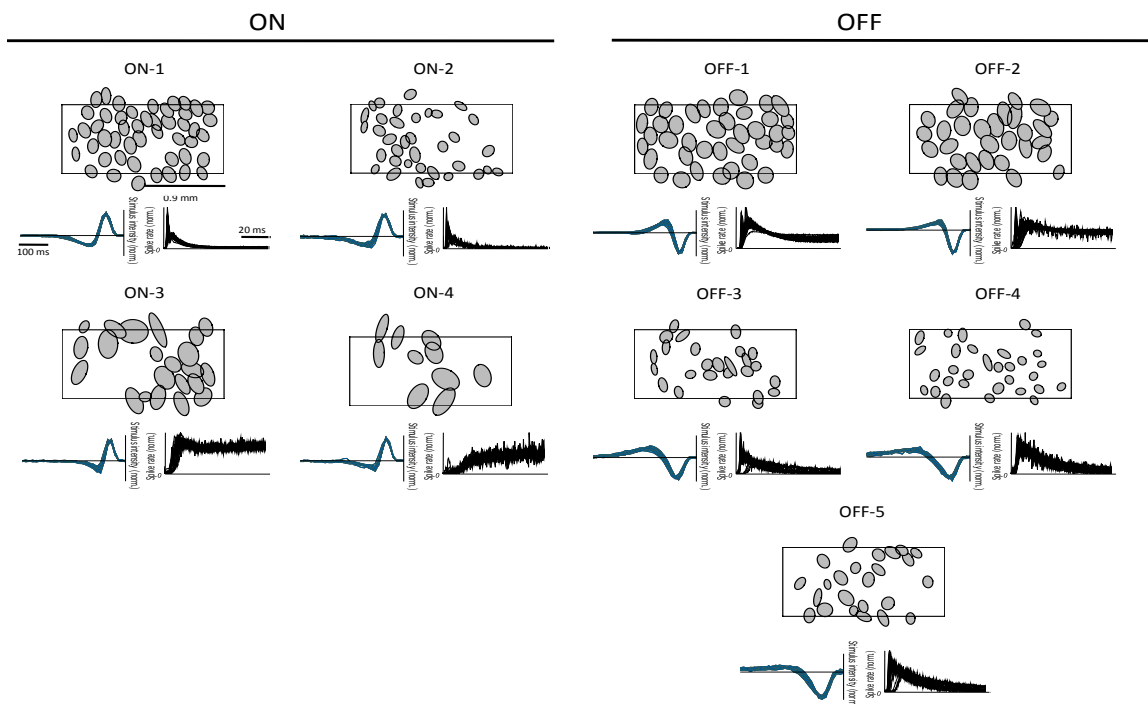
Wild-Type Rat RGC Classification #4
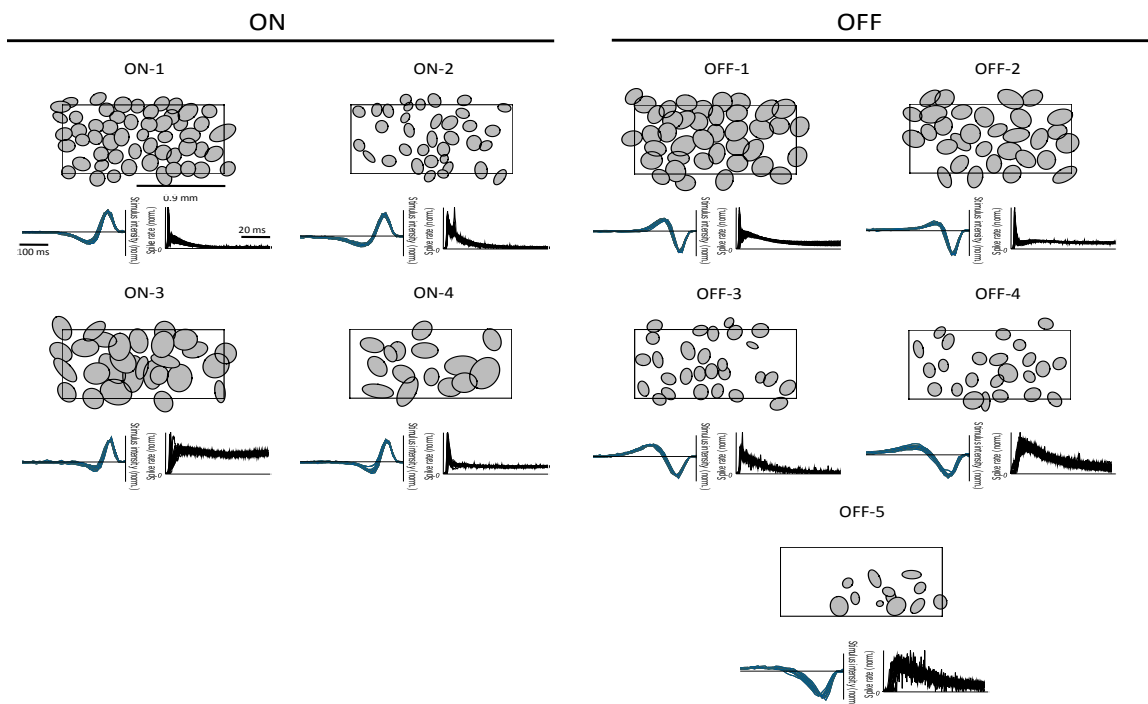
~4 Days Post-Optic Nerve Crush RGC Classification
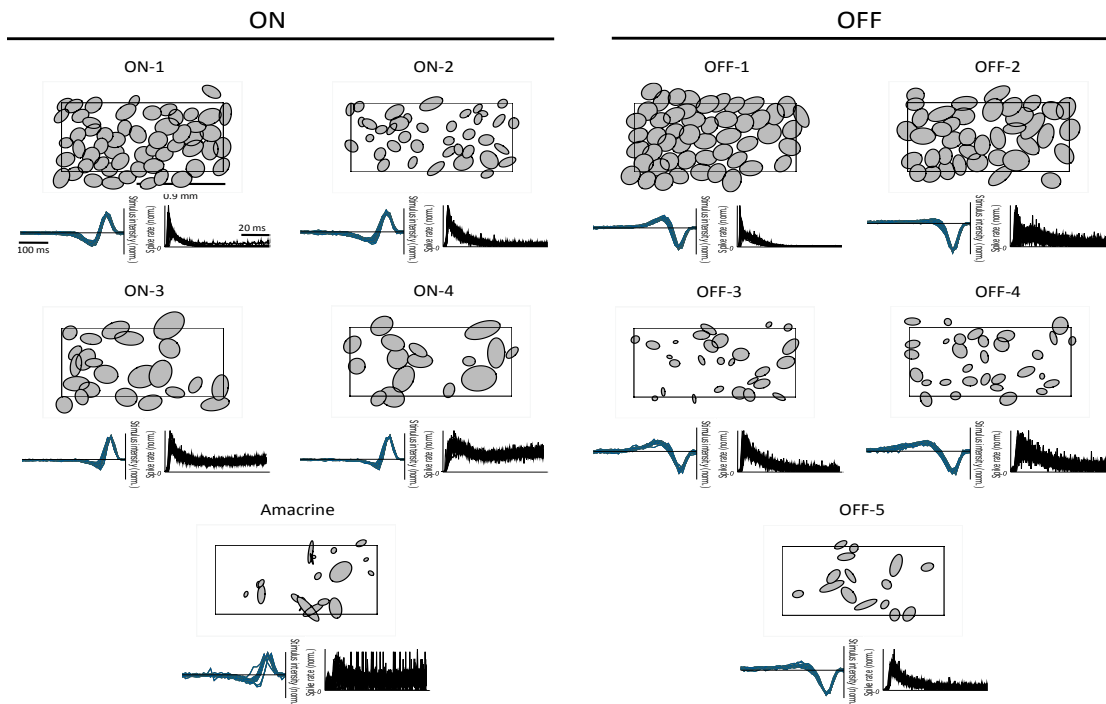
ON

ON-1

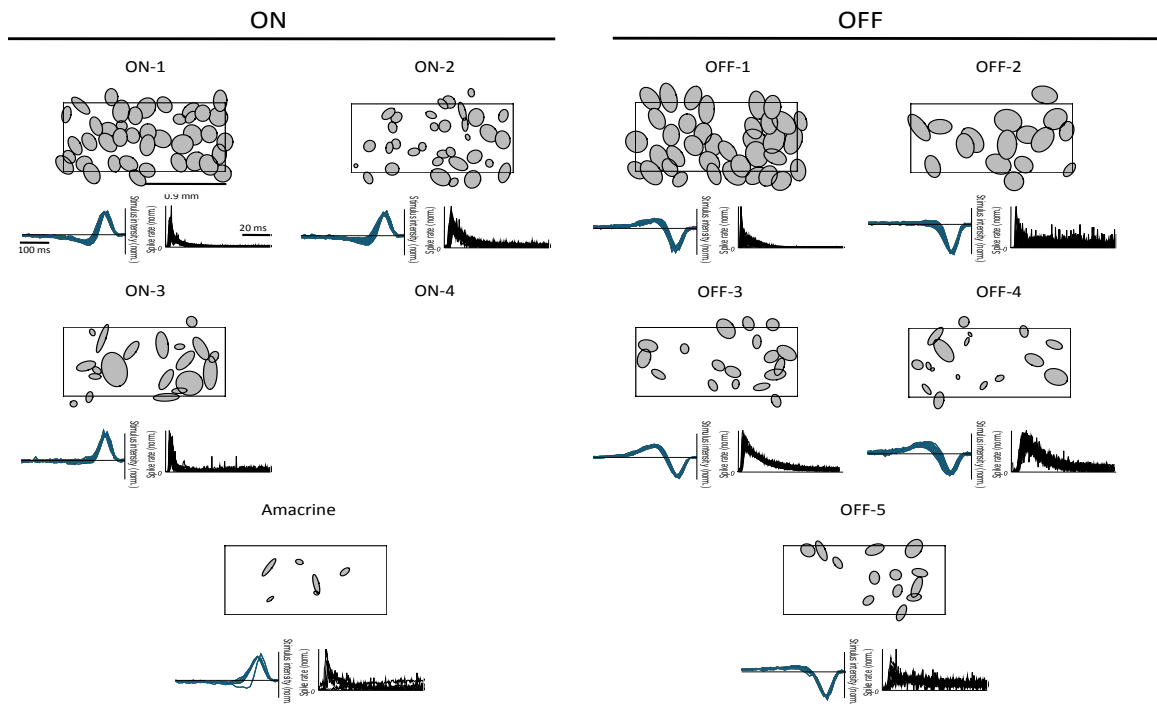0.9 mm

100 ms | 20 ms

ON-2

ON-3

ON-4

Amacrine

OFF

OFF-1

OFF-2

OFF-3

OFF-4

OFF-5

~7 Days Post-Optic Nerve Crush RGC Classification

ON

ON-1

0.9 mm

100 ms | 20 ms

ON-2

ON-3

ON-4

Amacrine

OFF

OFF-1

OFF-2

OFF-3

OFF-4

OFF-5

~7 Days Post-Optic Nerve Crush RGC Classification

ON

ON-1 ON-2

ON-3 ON-4

OFF

OFF-1 OFF-2

OFF-3 OFF-4

OFF-5

~8 Days Post-Optic Nerve Crush RGC Classification

ON

ON-1 ON-2

ON-3 ON-4

Amacrine

OFF

OFF-1 OFF-2

OFF-3 OFF-4

OFF-5

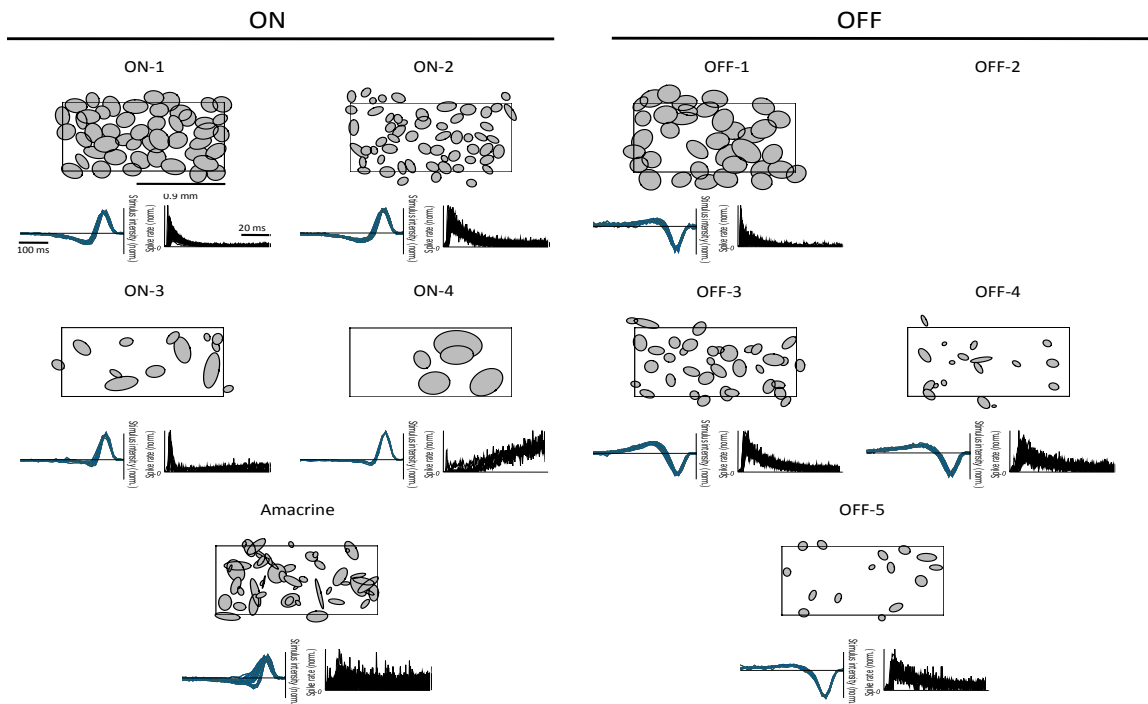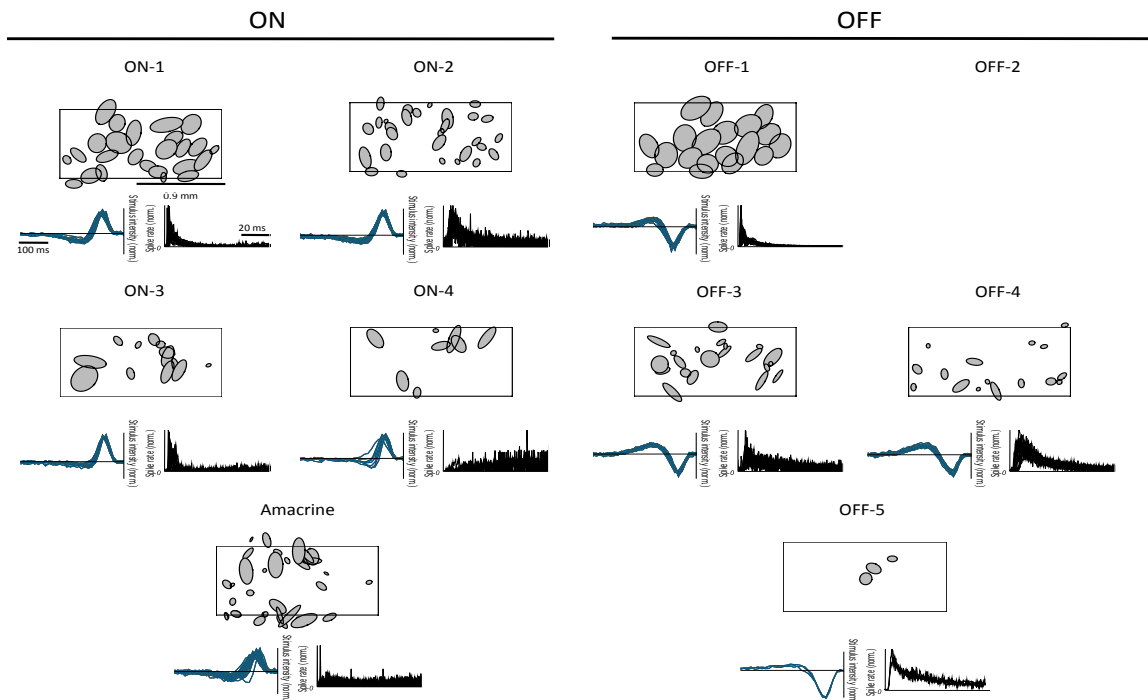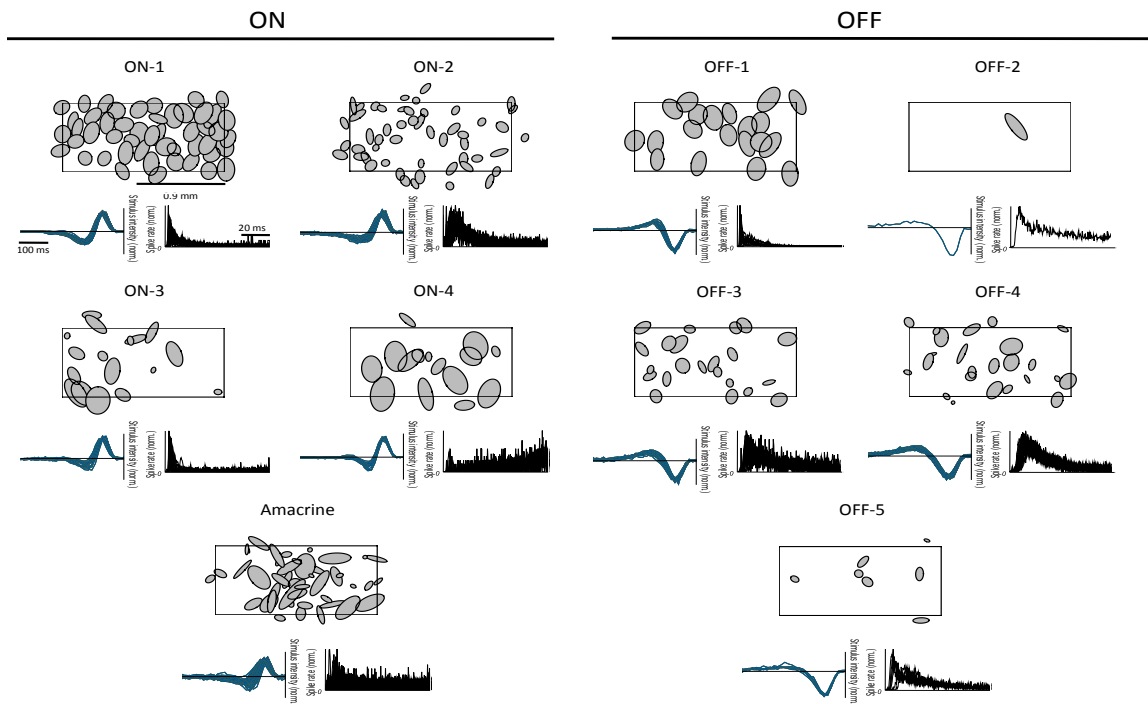# ~8 Days Post-Optic Nerve Crush RGC Classification
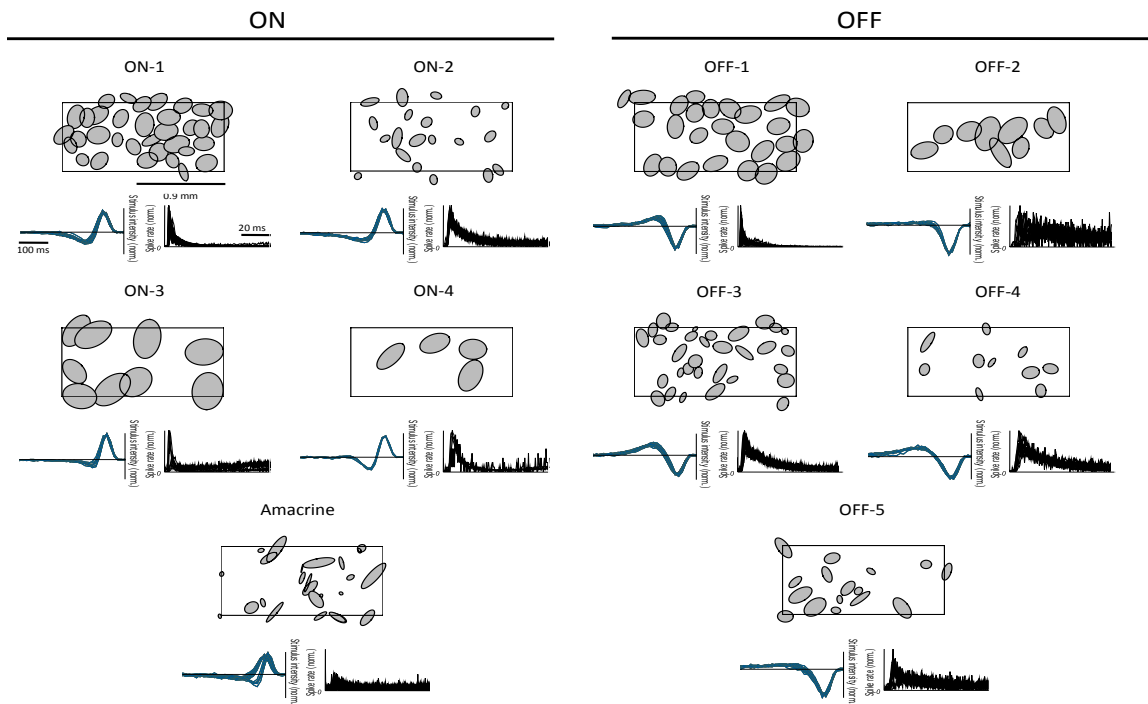
~8 Days Post-Optic Nerve Crush RGC Classification
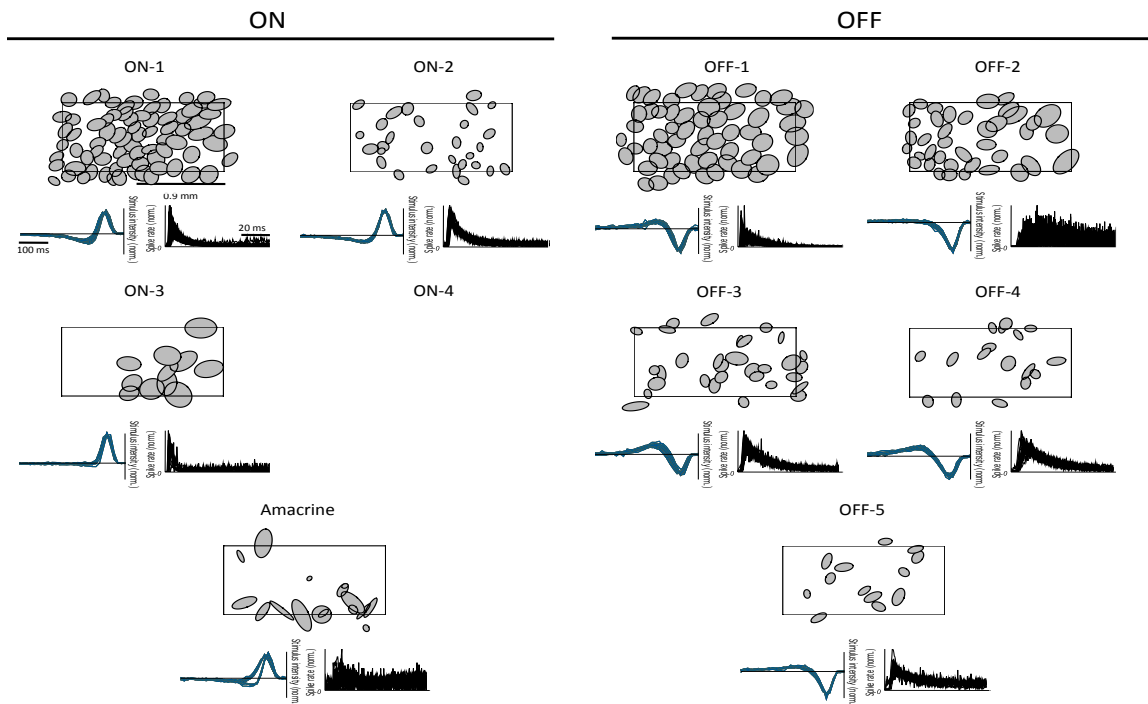
~8 Days Post-Optic Nerve Crush RGC Classification

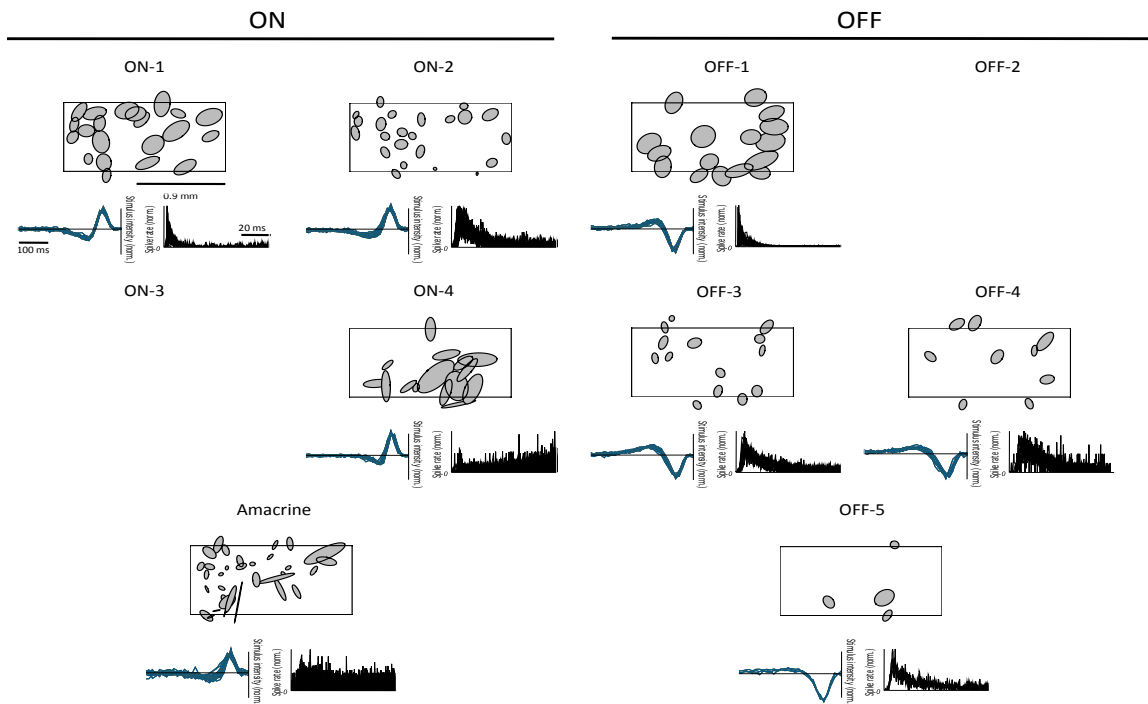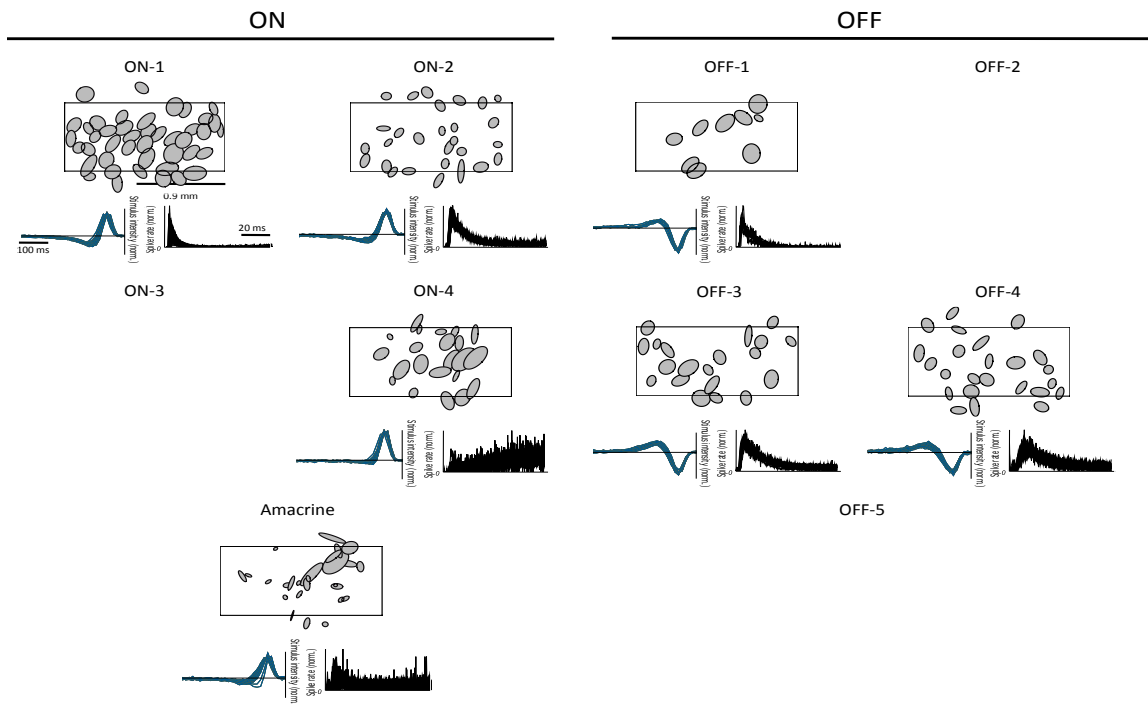~9 Days Post-Optic Nerve Crush RGC Classification

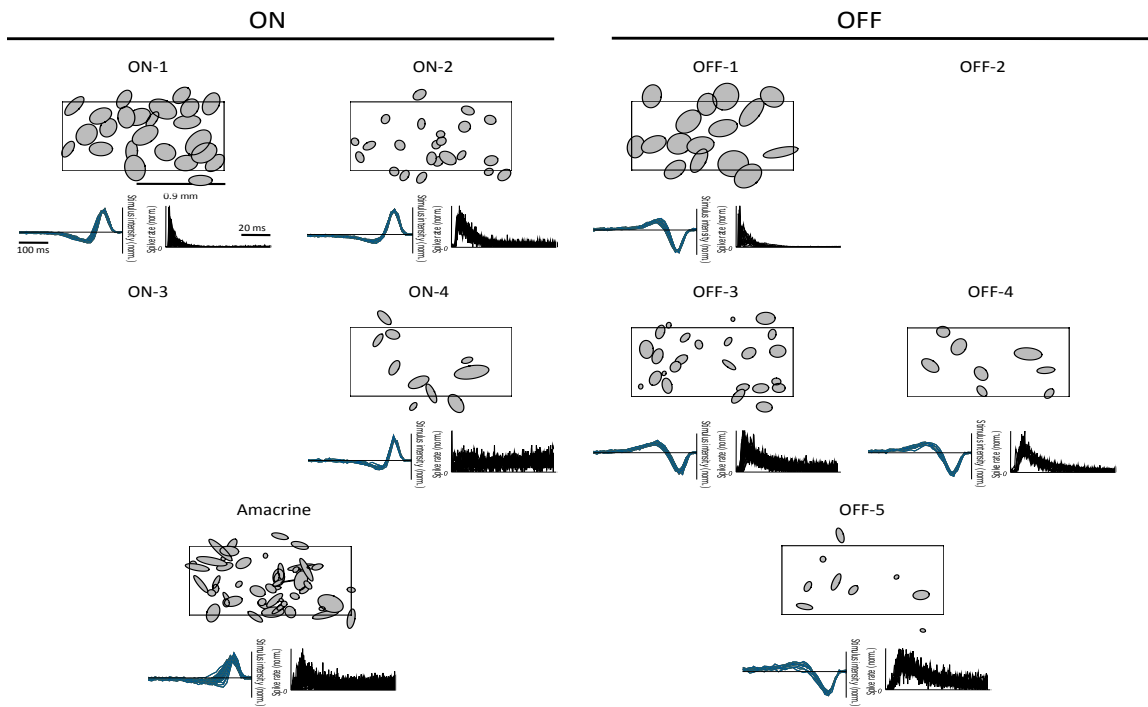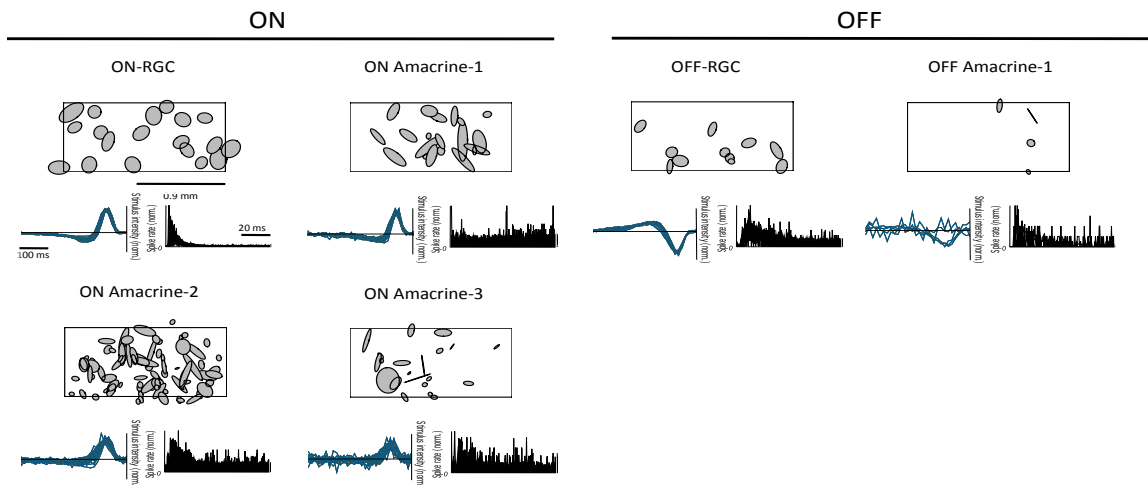## ~9 Days Post-Optic Nerve Crush RGC Classification

~10 Days Post-Optic Nerve Crush RGC Classification

~10 Days Post-Optic Nerve Crush RGC Classification
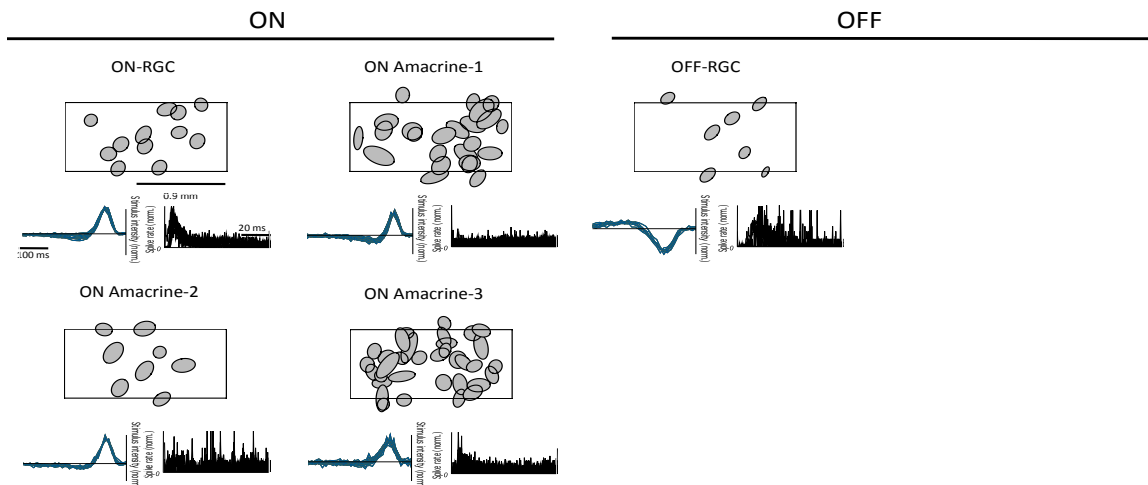
~11 Days Post-Optic Nerve Crush RGC Classification

~14 Days Post-Optic Nerve Crush RGC Classification

ON   ### OFF

ON-RGC   ON Amacrine-1   OFF-RGC   OFF Amacrine-1

ON Amacrine-2   ON Amacrine-3

~14 Days Post-Optic Nerve Crush RGC Classification

ON   ### OFF

ON-RGC   ON Amacrine-1   OFF-RGC

ON Amacrine-2   ON Amacrine-3

~15 Days Post-Optic Nerve Crush RGC Classification

ON

OFF

ON-RGC

ON Amacrine-1

OFF-RGC

OFF Amacrine-1

ON Amacrine-2

ON Amacrine-3
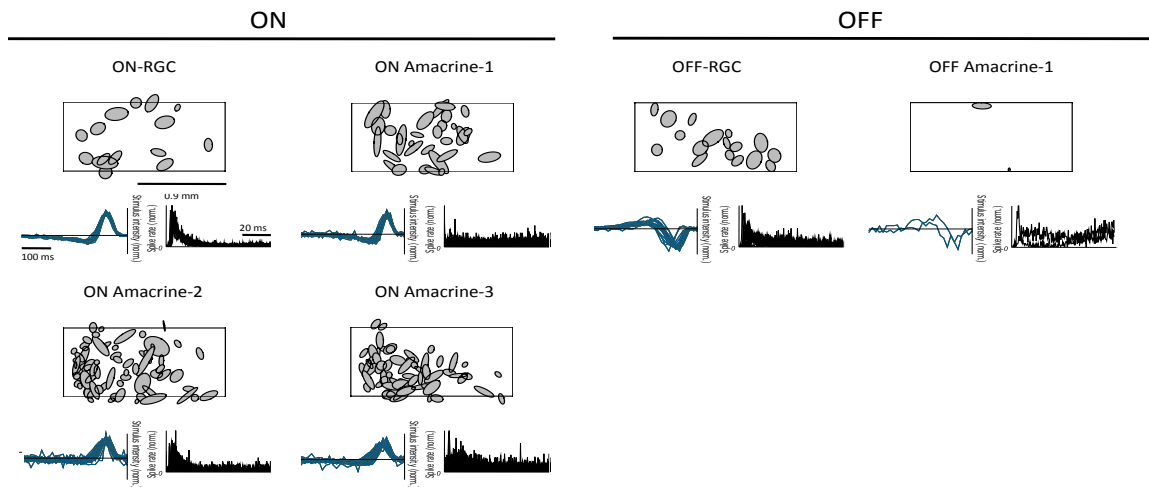
References

1. Weber AJ, Harman CD, Viswanathan S. (2008). Effects of optic nerve injury, glaucoma, and neuroprotection on the survivial, structure and function of ganglion cells in the mammalian retina. J Physiol. 586(18): 4393-4400

2. Gupta N, Yucel YH. (2007). Glaucoma as a neurodegenerative disease. Curr Opin Opthalmol. 18: 110-114.

3. Quigley HA. (2011). Glaucoma. Lancet. 377: 1367-1377.

4. Weinreb RN, Khaw PT. (2004). Primary open-angle glaucoma. Lancet. 363: 1711-1720.

5. Kumarasamy NA, Lam FS, Wang AL, Theoharides TC. (2006). Glaucoma: Current and Developing Concepts for Inflammation, Pathogenesis, and Treatment. Eur J Inflamm. 4(3): 129-137.

6. Rodieck RW. (1998). The first steps in seeing. Sunderland, MA: Sinauer.

7. Dacey D. (2004). Origins of Perception: Retinal Ganglion Cell Diversity and the Creation of Parallel Visual Pathways. The Cognitive Neurosciences. Cambridge, MA: MIT Press. 281-301.

8. Wong RC, Cloherty SL, Ibbotson MR, O'Brien BJ. (2012). Intrinsic physiological properties of rat retinal ganglion cells with a comparative analysis. J Neurophysiol. 108: 2008-2023.

9. Quigley HA, Sanchez RM, Dunkelberger GR, L'Hernault NL, Baginski, TA. (1987). Chronic Glaucoma Selectively Damages Large Optic Nerve Fibers. Invest Opthalmol Vis Sci. 28(6): 913-920.

10. Quigley HA, Dunkelberger, GR, Green, R. (1988). Chronic Human Glaucoma Causing Selectively Greater Loss of Larger Optic Nerve Fibers. Invest Opthalmol Vis Sci. 95: 357-363.

11. Glovinsky Y, Quigley HA, Dunkelberger GR. (1991). Retinal Ganglion Cell Loss Is Size Dependent in Experimental Glaucoma. Invest Ophthalmol Vis Sci. 32: 484-491.

12. Shou T, Liu J, Wang W, Zhou Y, Zhao K. (2003) Differential Dendritic Shrinkage of α and β Retinal Ganglion Cells in Cats with Chronic Glaucoma. Invest Opthalmol Vis Sci. 44(7): 3005-3010.

13. Feng L, Zhao Y, Yoshida M, Chen H, Yang JF, Kim TS, Cang J, Troy JB, Liu X. (2012). Sustained Ocular Hypertension Induces Dendritic Degeneration of Mouse Retinal Ganglion Cells that Depends on Cell Type and Location. Invest Ophthalmol Vis Sci. 54: 1106-1117.

14. Morgan JE, Uchida H, Caprioli J. (2000). Retinal ganglion cell death in experimental glaucoma. Br J Opthalmol. 84:303-310.

15. Osborne NN, Wood JO, Chidlow G, Bae JH, Melena J, Nash MS. (1999). Ganglion cell death in glaucoma: what do we really know? Br J Opthalmol. 83: 980-986.

16. Morgan JE. (1994). Selective cell death in glaucoma: does it really occur? Br J Opthalmol. 78: 875-880.

17. Litke AM, Bezayiff N, Chichilnisky EJ, Cunningham W, Dabrowski W, Grillo AA, Grivich M, Grybos P, Hottowy P, Kachiquine S, Kalmar RS, Mathieson K, Pterusca D, Rahman M, Sher A. (2004). What Does the Eye Tell the Brain?: Development of a System for the Large-Scale Recordings of Retinal Output Activity. IEEE Trans Nuck Sci. 51: 1434-1440.

18. Field GD, Sher A, Gauthier JL, Greschner M, Shlens J, Litke AM, Chichilnisky EJ. (2007). Spatial Properties and Functional Organization of Small Bistratified Ganglion Cells in Primate Retina. J Neurosci. 27(48): 13261-13272.

19. Kalenykas G, Oglesby EN, Zack DJ, Cone FE, Steinhart MR, Tian J, Pease ME, Quigley HA. (2012). Retinal Ganglion Cell Morphology after Optic Nerve Crush and Experimental Glaucoma. Invest Ophthalmol Vis Sci. 53:3847-3857.